Inorganic Chemistry

Article

pubs.acs.org/IC

Lanthanide Clusters with Azide Capping Ligands

Brian F. Moore, Thomas J. Emge, and John G. Brennan*

Department of Chemistry and Chemical Biology, Rutgers, the State University of New Jersey, 610 Taylor Road, Piscataway, New Jersey 08854-8087, United States

Supporting Information

ABSTRACT: Weakly binding azide ligands have been used as surface caps in the synthesis of lanthanide oxo and selenido clusters. Addition of NaN_3 and Na_2O to in situ prepared solutions of $Ln(SePh)_3$ in pyridine results in the formation of $(py)_{18}Sm_6Na_2O_2(N_3)_{16}$ or $(py)_{10}Ln_6O_2(N_3)_{12}(SePh)_2$ (Ln = Ho, Er), with the Sm and Er compounds characterized by low temperature single crystal X-ray diffraction. Attempts to prepare chalcogenido derivatives by ligand-based redox reactions using elemental Se were successful in the preparation of $(py)_{10}Er_6O_2(SeSe)_2(N_3)_{10}$, a diselenido cluster having crystallographic disorder due to some site sharing of both SeSe and N_3 ligands. These compounds all detonate when heated.

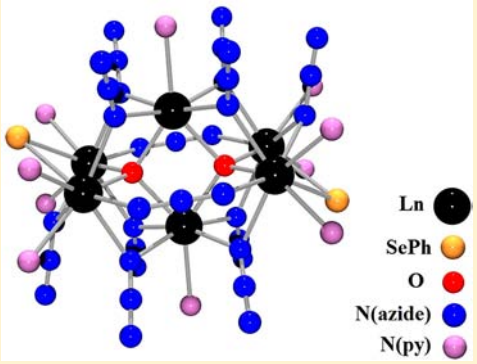

INTRODUCTION

The f-block nitrides (LnN, AnN) represent formidable synthetic challenges due to the chemical instability of a N^{3-} ion stabilized by essentially ionic interactions. Solid-state materials can be prepared at high temperatures, but molecular and cluster compounds with nitride ligands are exceptionally rare. In molecular chemistry, azide ligands are a potential source of nitrides because of their well-known tendency to eliminate N_2, so it is surprising to find that the chemistry of the f-block metals with azide ligands is relatively undeveloped. Initial studies focused primarily on coordination complexes[1−3] of $M(N_3)_x$ but the explosive nature of materials with high concentrations of azide ligands has certainly inhibited a systematic investigation into the reactivity of compounds with M−N_3 bonds. There is only one example of an f-element nitride cluster prepared from $M(N_3)_x$ starting materials, a tetrametallic uranium compound with a central tetrahedral N^{3-}.[4]

To better control this chemistry, there have been efforts devoted to the preparation of heteroleptic M−N_3 materials, typically with sterically demanding ancillary ligands.[5−11] These relatively unreactive ligands (i.e., amides, cyclopentadienides) lower the $[N_3]$ concentration that in turn reduces the shock/thermal instability of molecular products. As an added benefit, these ancillary ligands tend to form compounds that can be dissolved in apolar solvents, and this contributes additional stability because it becomes harder to stabilize polar reactive intermediates. With this additional control, molecular nitride compounds of the actinides have been described, first in the preparation of an octanuclear cluster with both azides and N^{3-} bridging Cp^*_2U,[12] and seven years later in the elegant preparation of a uranium molecule with a terminal U≡N bond.[13] The analogous lanthanide nitrides remain elusive.

In addition to their utility as nitride sources, azide ligands are also potentially useful in cluster chemistry. With lanthanides, similar weakly binding ligands [i.e., I,[14−16] EPh[17−27] (E = S, Se, Te)] have been used to prepare a variety of Ln oxide,[17−19] fluoride,[20] and chalcogenido[21−28] cluster compounds. Both EPh^- and I^- have a tendency to form soluble products with Ln(III) ions because the weak electrostatic forces that define M^+−X^- interactions are readily disrupted by Lewis base solvents ranging from pyridine to DME. Azides, with their single net-negative charge delocalized over two nitrogen atoms, offer a weaker Ln bonding interaction when compared with EPh^- and E^{2-} species while potentially forming soluble clusters with azides capping the cluster surface. This is an attractive prospect because in cluster syntheses, the identity of a crystalline cluster product is often influenced dramatically by the steric and electronic properties of the surface ligands,[27−34] and it is reasonable to expect that these weakly binding azides, with steric demands that fall between EPh and I, are likely to lead to the isolation of new cluster compounds.

Azide-capped clusters also represent an interesting class of starting materials for the preparation of molecular nitrides. High Ln concentrations are intrinsic properties of all cluster compounds, and this is ideally suited to providing the kinetic passivation that would be needed to stabilize a newly formed nitride anion before it can react further, that is, with solvents. These clusters could also be used to understand the properties of an emerging class of LnN_xO_y phosphors[35−40] by providing the spectroscopy community with atomically characterized materials to study. For these reasons, we have investigated the

Received: February 11, 2013
Published: May 2, 2013

   dx.doi.org/10.1021/ic400359x | Inorg. Chem. 2013, 52, 6021−6027

Table 1. Summary of Crystallographic Details for 1, 3, and 4

	compound		
	1	3	4
fw	3630.06	3275.84	2848.38
space group	$C2/c$	$P\text{-}1$	$P\text{-}1$
empirical formula	$C_{125}H_{125}N_{73}Na_2O_2Sm_6$	$C_{102}H_{100}Er_6N_{54}O_2Se_2$	$C_{65}H_{65}Er_6N_{39.07}O_2Se_{5.31}$
a (Å)	25.523(3)	14.307(1)	13.2354(8)
b (Å)	18.941(2)	15.587(1)	13.5062(8)
c (Å)	33.039(3)	16.380(2)	15.3672(9)
α (°)		115.349(2)	113.675(1)
β (°)	112.106(2)	103.765(2)	93.405(1)
γ (°)		104.963(2)	115.494(1)
V (Å^3)	14798(2)	2923.9(5)	2179.4(2)
Z	4	1	1
D (calcd) (g/cm^{-3})	1.629	1.860	2.170
temp (K)	100(2)	100(2)	100(2)
λ (Å)	0.71073	0.71073	0.71073
abs coeff (mm^{-1})	2.423	4.952	7.993
unique [$I > 2\ \sigma(I)$] reflns	122566	17615	13127
$R(F)^a$ [$I > 2\ \sigma(I)$]	0.0529	0.0296	0.0269
$R_w(F^2)^a$ [$I > 2\sigma(I)$]	0.1160	0.0628	0.0598

[a]Definitions: $R(F) = \Sigma||Fo| - |Fc||/\Sigma|Fo|$. $R_w(F^2) = \{\Sigma[w(Fo^2 - Fc^2)^2]/\Sigma[w(Fo^2)^2]\}^{1/2}$. Additional crystallographic details are given in the Supporting Information.

use of azide ligands in Ln cluster chemistry, and we report here our initial findings.

EXPERIMENTAL SECTION

General Methods. All syntheses were carried out under ultrapure nitrogen (Welco Praxair), using conventional drybox or Schlenk techniques. Ln metals, Se, Na_2O (Strem), and Hg (Aldrich) were purchased and used as received. NaN_3 (Aldrich) was dried in vacuo at room temperature for 12 h prior to use. Pyridine and hexanes (Aldrich) were purified with a dual column Solv-Tek solvent purification system and collected immediately prior to use. PhSeSePh (Strem) was purchased and recrystallized from hexane. Melting points were recorded in sealed capillaries and are uncorrected. FTIR spectra were recorded on a Thermo Nicolet Avatar 360 FTIR spectrometer from 4000 to 450 cm^{-1} as Nujol mulls on CsI plates. Nujol was added first, followed by the addition of product before grinding the product to a powder. Elemental analyses were performed by Quantitative Technologies, Inc. (Whitehouse, NJ). All these products lose lattice and coordinated solvent to form amorphous materials within minutes of isolation from solution, and this tends to give combustion analyses for C, H, and N that are lower than the calculated values. All the products detonate violently when heated, to the extent that the minute quantities used in melting point determinations will shatter the sealed capillary container, and this also impacts on the experimentally determined amount of nitrogen in the sample.

Caution: Lanthanide oxyazide and lanthanide oxychalcogenido azide clusters are potentially hazardous, moisture-sensitive materials with explosive tendencies at elevated temperatures through detonation (sonic wave propagation) and deflagration (fire propagation) processes. Appropriate safety precautions such as a face shield, Kevlar gloves, and Teflon spatulas should be employed; pure materials should not be produced in amounts greater than 100 mg.

(1). Synthesis of $(py)_{18}Sm_6O_2(N_3)_{16}Na_2$ 7(py). Sm (160 mg, 1.06 mmol), Hg (39 mg, 0.19 mmol), and diphenyl diselenide (478 mg, 1.53 mmol) were combined in pyridine (30 mL), and the mixture was stirred for 24 h to give a clear light orange solution. Sodium azide (137 mg, 2.10 mmol) and sodium oxide (63 mg, 1.01 mmol) were then added, and the mixture was stirred for 3 days in a dark environment to give a clear yellow solution and a white precipitate. The solution was filtered, concentrated to 20 mL, and layered with hexanes (4 mL) in the dark to give hexagonal colorless crystals (46 mg, 8.3%) that become white and amorphous when removed from mother liquor, turn brown at 119 °C, and detonate at 295 °C. IR: 3080 (m), 2962 (s), 2796 (m), 2662 (w), 2495 (m), 2357 (s), 2339 (m), 2132 (w), 2115 (w, bridging azide), (terminal) 2052 (m), 1941 (m), 1580 (m), 1437 (m), 1340 (w), 1261 (w), 1029 (w) cm^{-1}. Anal. Calcd for $C_{125}H_{125}N_{73}Na_2O_2Sm_6$ (with values for material with no lattice solvent in parentheses): C, 41.3 (35.0); H, 3.47 (2.94); N, 28.2 (30.4). Found: C, 32.9; H, 2.31; N, 24.2.

(2). Synthesis of $(py)_{10}Ho_6O_2(N_3)_{12}(SePh)_2$ 8(py). Diphenyl diselenide (650 mg, 2.08 mmol), Hg (17 mg, 0.084 mmol), and Ho (333 mg, 2.01 mmol) were combined in pyridine (25 mL), and the mixture was stirred for 24 h to give a clear dark brown solution with no visible metal. Sodium azide (65 mg, 1.05 mmol) and sodium oxide (68 mg, 1.10 mmol) were then added, and after stirring for 72 h, the opaque reddish brown solution was filtered (20 mL), concentrated (18 mL), and layered with hexanes (3 mL) in the dark to give faint pinkish micro crystals (251 mg, 34%) that become opaque when removed from solvent, and detonate at 310 °C. IR: 2962 (m), 2905 (w), 2498 (w), 2351 (w), 2121 (w, bridging azide), 2053 (m, terminal azide), 1941 (w), 1260 (s), 1091(s), 1018 (s), 799 (s) cm^{-1}. Anal. Calcd for $C_{102}H_{100}N_{54}Se_2O_2Ho_6$: C, 37.6; H, 3.09; N, 23.2. Found: C, 36.7; H, 3.20; N, 20.6.

(3). Synthesis of $(py)_{10}Er_6O_2(N_3)_{12}(SePh)_2$ 8(py). Diphenyl diselenide (630 mg, 2.01 mmol) and Hg (420 mg, 2.09 mmol) were combined in pyridine (40 mL), and the mixture was stirred for 24 h to give a clear yellow solution. Er (178 mg, 1.06 mmol) was added, and after 14 h, sodium azide (65 mg, 1.00 mmol) and sodium oxide (73 mg, 1.17 mmol) were added. After 2d, the opaque greenish gray mixture was filtered to give a yellow solution that was concentrated (10 mL) and layered with hexanes (3 mL) in the dark to produce faint purple crystals (90 mg, 15%) that degrade at 85 °C, further degrade into a brown amorphous powder at 270 °C, and detonate at 336 °C. IR: 3699 (m), 3077 (m), 3024 (m), 2662 (w), 2499 (w), 2361 (w), 2125 (m, bridging azide), 2054 (m, terminal azide), 1944 (w), 1580 (s), 1481 (m), 1437 (m), 1260 (w), 1146 (w), 1030 (m), 990 (m), 747 (m), 703 (s), 602 (m) cm^{-1}. Anal. Calcd for $C_{102}H_{100}N_{54}Se_2O_2Er_6$: C, 37.4; H, 3.08; N, 23.1. Found: C, 34.5; H, 3.60; N, 17.5.

(4). Synthesis of $(py)_{10}Er_6O_2(Se_2)_{2+x}(N_3)_{10-2x}$ 3(py). Cd (110 mg, 2.09 mmol) and diphenyl diselenide (1300 mg, 4.16 mmol) were combined in pyridine (50 mL) while stirring for 24 h to give a dark yellow, clear solution. Er (167 mg, 1.00 mmol) and Hg (50 mg, 0.25

dx.doi.org/10.1021/ic400359x | Inorg. Chem. 2013, 52, 6021−6027

mmol) were added to the solution, and after stirring for 5 h, the dark yellow-green solution was filtered to remove a gray precipitate. Elemental Se (160 mg, 2.02 mmol), sodium azide (65 mg, 1.05 mmol), and sodium oxide (63 mg, 1.01 mmol) were then added, and after 2 days, the dark red solution was filtered to remove the yellow precipitate that had formed. Layering with hexanes in the dark gave pink-orange plates (60 mg, 4.2%) that flash and detonate at 312 °C. IR: 2962 (s), 2904 (m), 2659 (w), 2354 (w), 2107 (m, bridging azide), 2082 (m, terminal azide), 2057 (w, terminal azide), 1945 (m), 1598 (m), 1440 (m), 1412 (m), 1260 (s), 1020 (s), 865 (m), 798 (s), 701 (s) cm^{-1}. Anal. Calcd for $C_{65}H_{65}N_{39}Se_{5.3}O_2Er_6$: C, 27.4; H, 2.30; N, 19.2. Found: C, 26.6; H, 2.00; N, 16.3.

X-ray Structure Determination. Data for **1**, **2**, **3**, and **4** were collected on a Bruker Smart APEX CCD diffractometer with graphite monochromatized Mo Kα radiation (λ = 0.71073 Å) at 100 K. Crystals were immersed in Paratone oil and examined at low temperatures. Single crystal X-ray data for **2** verified its crystal structure to be isostructural to that of **3**. All X-ray data were corrected for Lorenz effects, polarization, and absorption, the latter by a multiscan (SADABS)[41] method. The structures were solved by direct methods (SHELXS86).[42] All non-hydrogen atoms were refined (SHELXL97)[43] on the basis of F_{obs}^2. All hydrogen atom coordinates were calculated with idealized geometries (SHELXL97). Scattering factors (f_o, f', f'') are as described in SHELXL97. Crystallographic data and final R indices for **1**, **3**, and **4** are given in Table 1. POVRAY diagrams[44] for **1**, **3**, and **4** are shown in Figures 1, 2, and 3, respectively, with selected bond distance summaries given in the figure captions. Complete crystallographic details are given in the Supporting Information.

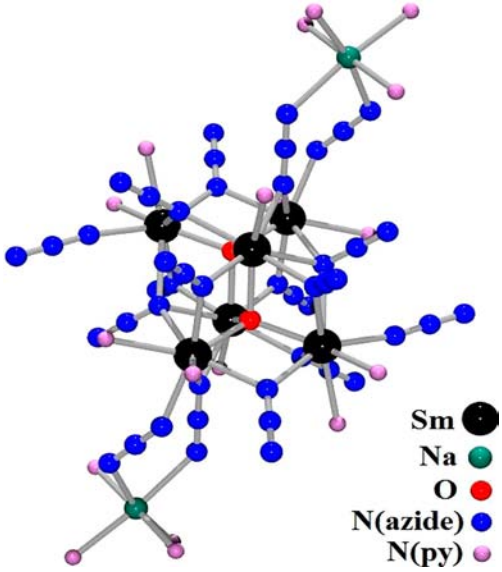

Figure 1. The core region of the $(py)_{18}Sm_6O_2(N_3)_{16}Na_2$ molecules of **1**, with H and C atoms removed for clarity. Bond distance ranges (Å, with average ESD in parentheses) for **3**: Sm−O 2.289−2.316(3), Sm−N(azido, EO bibridged) 2.435−2.580(4), Sm−N(azido, EO tribridged) 2.603−2.847(4), Sm−N(azido, EO terminal) 2.371(5), Sm−N(py) 2.611−2.684(5), and Na−N(py) 2.443, 2.601(7).

Thermolysis. Crystalline **1** (4 mg) was placed in custom-made, L-shaped, 5- and 10-mm-diameter quartz tubes with 39.5 and 22.5 cm of length before and after the bend, respectively. The tubes were then sealed under vacuum with the sample end of the tube in the oven. The temperature of the oven was raised quickly (20 °C/min) until it was stabilized at 650 °C, and was kept at this temperature for 5 h. The other end of the thermolysis tube was kept in liquid nitrogen during the experiment. Black powders formed, and a powder diffraction pattern (PXRD) obtained by use of the Bruker HiStar area detector mounted on a rotating-anode generator with a Cu target monochromatized with Rigaku Osmic mirrors (λ = 1.5418 Å)

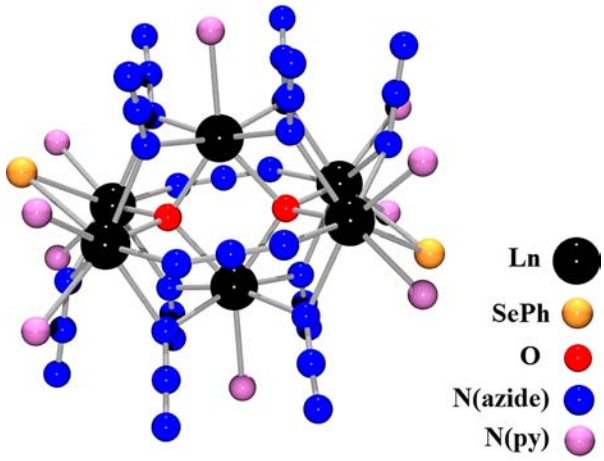

Figure 2. The central "core" region of $(py)_{10}Ln_6O_2(N_3)_{12}(SePh)_2$, with H and C atoms removed for clarity. Bond distance ranges (Å, with average ESD in parentheses) for **3** (Ln = Er): Er−O 2.235−2.254(2); Er−N(u_2 azido, EO) 2.382−2.458(3); Er−N(azido, EE bibridged) 2.446, 2.463(3); Er−N(py) 2.494−2.628(3); and Er−Se 2.9471, 2.9589(4).

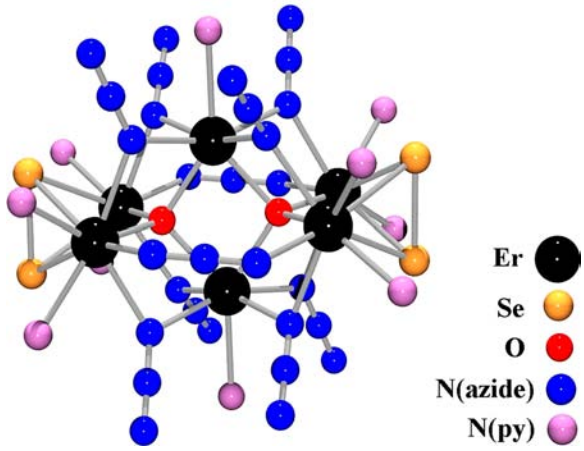

Figure 3. The core region of the $(py)_{10}Er_6O_2(Se_2)_{2+x}(N_3)_{10-2x}$, with x = 0 (e.g., major site constituents) and the H and C atoms removed for clarity. Bond distance ranges (Å, with average ESD in parentheses): Er−O 2.240−2.263(2); Er−N (azido, EO bibridged) 2.357−2.454(3); Er−N(azido, EE bibridged) 2.422, 2.472(4); Er−N(py) 2.509−2.609(3); Er−Se (site 100% occupied)) 2.8767−2.9260(4); Er−Se (site 28% occupied) 2.850−3.138(2); and Er−Se (sites 3% occupied) 2.80−3.39(2).

revealed that Sm_2O_3, PDF 00-015-0813 (ICDD, 2003) was present. The above process was repeated for crystalline **3** (4 mg). The PXRD pattern of it, a thermolysis product, also a black powder, revealed that Er_2O_3, PDF 00-026-0604 (ICDD, 2003) was present.[45] The cold part of the thermolysis tube for **3** was washed with acetonitrile and then analyzed by GC/MS spectrometry to identify Ph_2Se as the only volatile product of the reaction.

RESULTS AND DISCUSSION

Initial efforts focused on the synthesis of clusters with oxo ligands because of the interest in using lanthanide oxynitrides as phosphor materials,[35−40] and $Ln(SePh)_3$ was chosen as a starting material to prepare heteroleptic $Ln(N_3)_x(SePh)_{3-x}$ in situ that could then be treated further with elemental chalcogen. Initial results show that azide ligands will encapsulate a range of oxo cluster materials, with the oxo

dx.doi.org/10.1021/ic400359x | Inorg. Chem. 2013, 52, 6021−6027

ligand most conveniently introduced using Na_2O, because water, either serendipitously introduced from hydroscopic NaN_3 reagents or deliberately introduced as THF solutions, gave nonreproducible products. Addition of Na_2O and NaN_3 to a solution of in situ-prepared $Sm(SePh)_3$ (reaction 1), followed by filtration and saturation, leads to the selective precipitation of hexanuclear $(py)_{18}Sm_6Na_2O_2(N_3)_{16}$ (**1**).

$$Sm(SePh)_3 + Na_2O + NaN_3 \xrightarrow{py} (py)_{18}Sm_6Na_2O_2(N_3)_{16} \quad (1)$$

Cluster **1** was characterized by low-temperature single-crystal X-ray diffraction. The structure contains a 2D polymeric network of hexametallic samarium oxo clusters, represented in Figure 1, which shows a POVRAY[44] diagram of the repeating chemical unit. In the product, six Sm are connected by two oxo dianions with coordination environments that are slightly distorted from ideal tetrahedral geometries. This core Sm_6O_2 unit is capped by a pair of $(py)_3Na$, and these $Na_2Sm_6O_2$ clusters are connected in a 2D polymeric network via the pair of $(py)_3Na$ linking groups that have two azido ligands bridging to one adjacent cluster and one azido ligand to another cluster in an approximately orthogonal direction. As observed in several metal azido $(M_x(N_3)_y)$ compounds with $x \geq 4$, there are three modes of bridging for the N_3 ligands: namely, "end-only" (EO) and doubly or triply bridging "end-to-end" (EE), as described by Ribas in 1999.[46]

The azides in **1** adopt terminal, doubly, or triply bridging motifs, and there are also EE N_3's that bridge Sm and Na. The details for the metal-to-ligand bond lengths in **1** can be summarized as follows: 2.28−2.32 Å for the eight unique Sm−O's, which are consistent with the examples in the Cambridge Structural Database (CSD);[47−49] 2.44−2.58 Å for the 16 Sm−N's from bridging EO azido ligands; 2.42−2.44 Å for the Sm−N's from the linking EE azido ligand; 2.50−2.60 Å for the Sm−N's from linking azido ligand with EE mode to a second Sm atom and EO mode to a third Sm atom; 2.60−2.85 Å for the 6 Sm−N's from the triply bridging EO azido ligands; 2.61−2.68 Å for the 10 Sm−N's from py ligands; 2.42−2.62 Å for the 7 Na−N(py)'s, with the two largest, 2.52 and 2.62 Å from the linking $(py)_3Na(N_3)_3$ group, as expected, based on likely steric effects at the polymerization site; and 2.48−2.60 Å for the Na−N's from the 5 EE azido that link to Sm atoms. Overall, the Sm−N distances for bridging azido ligands are consistent with the few examples in the CSD.[8,9] The regularity of all Sm−O and Sm−N(py) distances reflects the limited variation of Sm coordination environments, which are all 8-coordinate.

Under similar conditions (reaction 2), the smaller lanthanides Ho and Er gave the related hexanuclear azide selenolates $(py)_{10}Ln_6O_2(N_3)_{12}(SePh)_2$ (Ln = Ho(**2**), Er(**3**)).

$$Ln(SePh)_3 + Na_2O + NaN_3 \xrightarrow{py} (py)_{10}Ln_6O_2(N_3)_{12}(SePh)_2 \quad (Ln = Ho(2), Er(3)) \quad (2)$$

The structures of **2** and **3** have also been determined by X-ray diffraction at low temperature; a POVRAY diagram of **3** is given in Figure 2. The structure of **2** was determined to be isostructural to that of **3** by use of the low-temperature X-ray data. These compounds have approximately C_{2v} site symmetry, with two kinds of azido bridges and two crystallographically identical oxo atoms that are found on opposite sides of the inversion center that is the molecular center of mass, making the overall molecular cluster ellipsoidal in shape. The internal Ln_6O_2 core of cluster **2** or **3** is nearly identical to the core found in **1**: 8 of the 10 bonded py ligands are located at the two ends and impart a slight "hourglass" shape to the molecule, a characteristic that is not favorable for optimum crystal packing, so that many (in this case, 8) py of solvation are required to maintain efficient packing. Also at the surfaces of **2** and **3** are the selenolato ligands with the phenyl groups folded inward to conserve on molecular volume. This would likely aid in efficient packing of the molecules versus a more extended configuration for the selenolato ligands, as observed in the terminal SePh ligands for a range of multimetallic compounds, that is, in $(py)_2Yb(SePh)_4Li(py)_2$,[50] $(py)_8Yb_4Se_4(SePh)_4^f$[51] or $(py)_8Yb_4Hg_2Se_6(SePh)_4$.[23]

The oxo O atoms in **2** and **3** are 4-coordinate and create two off-center Ln_4O tetrahedral core units that share one edge. Of the 60 examples of crystal structures containing $(Ln)_xO$ with $x \geq 4$ and with 4-coordinate O atoms in the CSD, over 40 have this approximately tetrahedral[52−61] Ln_4O, rather than square planar, pyramidal, or distorted bipyramidal geometries. Similar variations in lanthanide oxo- and hydroxyl-containing cluster coordinations were discussed in detail by Junk.[62]

The phenylselenolato ligands in **2** and **3** are doubly bridging, which is the most common bonding motif for SePh in lanthanide clusters.[63−66] To complete the coordination spheres of the 6 Ln, there are 10 neutral py ligands. Terminal N_3 or SePh ligands, while frequently found in other azido and selenolato Ln clusters, are not nearly as prevalent as the bridging species in the Ln_6O_2 azido structures presented here.

In the structures of **2** and **3**, there are two different coordination schemes to the three independent Ln ions. The first two Ln's are 8-coordinate with a square antiprismatic arrangement of the bonded atoms: one O, one Se, and six N atoms, the latter from three EO doubly bridging azidos, one doubly bridging EE azido, and two terminal py ligands. The third unique Ln atom is 7-coordinate with an approximate pentagonal bipyramidal arrangement of the bonded atoms: two O's, four N's from EE azido only, and one terminal py. The coordination of the two centrally located O atoms and the six Ln atoms here can be clearly seen in Figure 2. The proximity of different Ln atoms to the center (X) of the cluster is clearly shown in Figures 1−3 and is quantified for **2** with two "outer" Ln's having a Ho···X of 3.29 Å, and one "inner" Ho···X of 1.79 Å. For isostructural **3**, the corresponding Er···X distances are 3.29 and 3.28 Å for the "outer" Ln and 1.78 Å for the "inner" Ln. It first appears unusual that the "inner" Ln in **2** or **3**, which is closest to the centroid of the molecule, has the lower coordination number; however, the core of the molecule is concentrated with Ln and O atoms, as depicted by an edge-sharing pair of Ln_4O tetrahedra in Figures 1−3, and this edge involves only the "inner" Ln and its inversion mate. Thus, there is a lower coordination number for the "inner" Ln as a result of the shortage of possible ligands in the concentrated core of the molecule.

Addition of elemental chalcogen to these preparations leads to the isolation of chalcogenido clusters, although the chemistry is not straightforward. With selenium, a diselenide product for Ln = Er could be obtained only when $Cd(SePh)_2$ was present in solution. In this case, hexanuclear $(py)_{10}Er_6O_2(Se_2)_2(N_3)_{10}$ (**4**) was isolated in small yield (reaction 3). The molecular structure of **4** is illustrated with a POVRAY diagram in Figure 3.

dx.doi.org/10.1021/ic400359x | Inorg. Chem. 2013, 52, 6021−6027

$$Cd(SePh)_2/Er(SePh)_3 + NaN_3 + Na_2O + Se \xrightarrow{py} (py)_{10}Er_6O_2(Se_2)_2(N_3)_{10} \quad (3)$$

The fact that the cadmium selenolate influences the identity of the isolated product, while not understood on a molecular level in this case, is entirely consistent with prior work. Lanthanide chalcogenolates have long been known to react with main group chalcogenolates[25,67−73] to form two types of heterometallic compounds, either discrete molecules with Ln−E(R)−M connectivities or ionic products in which the main group metal abstracts ER from Ln to give salts with Ln cations and $M(ER)_x$ anions. In the present system, this shift in solution speciation is clearly important to product identity because the presence of $Cd(SePh)_2$ is necessary for the isolation of **4**, and it should also be noted that **4** does not form when the Cd compound is replaced with either $Zn(SePh)_2$ or $Hg(SePh)_2$. The coordination geometries for the three unique Er atoms in **4**, with respect to the azido and py ligands, are quite similar to those of **1** and **2**: 2.24−2.26 Å for the 8 unique Er−O's; 2.36−2.45 Å for the 8 Er−N's from μ_2 bridging EO azido ligands; 2.42 and 2.47 Å for the Er−N's from the linking EE azido ligand; and 2.51−2.61 Å for the 5 Er−N's from py ligands.

The crystal structure of **4** contains evidence of site disorder in some ligands, namely, the substitution of diselenido ligands for pairs of azido ligands for a small fraction (<3%) of unit cells for two sites and, to a greater degree (28%), at a third site. Since in each of these three sites, the central EE azido ligand would be one of the pair removed, the substitutions to these sites are mutually exclusive.

The bonding geometries of the diselenido ligands to Er include Er−Se distances of 2.88−2.93 Å for bonds to the fully occupied diselenido ligand, which has a Se−Se bond length of 2.37 Å. In comparison, there are Er−Se distances of 2.8−3.1 Å for the partially occupied diselenido ligands, which have an average Se−Se distance of 2.4 Å. These Er−Se distances are all consistent with previously reported values for other Er diselenide structures.[74] The lanthanide distances to N atoms of EE azido ligands seem to be constant at 2.45, apparently the result of strain and steric effects rather than differences in Ln radius.

Although very similar, the azide bridging modes displayed in **1**−**4** show subtle variations. In all four products, two azido bridging modes (doubly bridged EE and EO) are present. The azidos are relegated to the cluster surfaces and display nearly identical bond lengths; however, the bridging modes of **1** and those of **2**−**4** diverge slightly because of the presence of the Ln−Ln EE bridging mode. This mode is absent in **1**, with only a Na−Ln EE bridge. This can be explained by the smaller ionic radii of Er^{3+} and Ho^{3+} in **2**−**4** when compared with the appreciably larger radii of Sm^{3+} as well as the presence of Na in **1**.

Attempts to explore the thermolysis of pure crystalline cluster compounds were frustrated by the tendency of these materials to detonate with elimination of N_2. In each attempt, pyrolysis resulted in explosion (**2**, **3**, and **4**) or deflagration (**1**) events. The powder diffraction of the resultant solid−state products revealed only the presence of microcrystalline oxide products, with no evidence for the formation of metal nitrides or ternary products. Solution pyrolysis, which offers a greater degree of kinetic control, are clearly warranted.

The reactivity as well as the weakly binding nature of the N_3^- ligand readily supports the observed microanalytical data as well as the isolated pyrolysis products. The photoreactivity of terminal M−N_3 bonds have been explored by Kiplinger[75] and Sadler.[76] In each case, azide degradation to N_2 was induced under ambient visible light exposure. In addition, the weak binding of azide anions and rapid crystal deliquescence of chalcogenide azide systems have been documented by Klapotke.[77] Compounds **1**−**4** readily experienced crystal degradation upon removal from solvent as well as unavoidable ambient light exposure during elemental analysis. Subsequently, the analytical data values obtained were consistent with the loss of py and azido ligands in each product. This point is particularly applicable in the case of **1** for which the number of coordinated pyridines and azides (18 py and 16 N_3) were appreciably greater than in **2**−**4**. This resulted in elemental values with significant deviations from the expected ranges for solvent-only loss. Finally, the isolation of oxide pyrolysis products can be rationalized by a significant loss of azido ligands (N_2 expulsion) and the presence of comparatively stronger coordinating Ln−O interactions in the product cores producing the more thermodynamically favored oxide products.

CONCLUSION

Lanthanide azide cluster materials with oxo and chalcogenido ligands can be prepared from lanthanide chalcogenolate starting materials. In all cases, the highly charged group 16 elements become the core anions, with azides decorating the cluster surfaces. These materials become increasingly stable as the ratio of N_3/Ln decreases. Experiments to establish the utility of these compounds as starting materials for the solution phase preparation of nitride or oxynitride clusters are currently underway.

ASSOCIATED CONTENT

Supporting Information

X-ray crystallographic files in CIF format for the crystal structures of **1**, **2**, **3**, and **4**. This material is available free of charge via the Internet at http://pubs.acs.org.

AUTHOR INFORMATION

Corresponding Author

*E-mail: bren@rci.rutgers.edu.

Notes

The authors declare no competing financial interest.

ACKNOWLEDGMENTS

This work was supported by NSF (CHE-0747165).

REFERENCES

(1) Kou, H. Z.; Liao, D. Z.; Cheng, P.; Jiang, Z. H.; Yan, S. P.; Want, G. L. *Synth. React. Inorg. Met.-Org. Chem.* **1998**, *28*, 405−414.
(2) Starynowicz, P.; Bukietynska, K.; Ryba-Romanowski, W.; Dominiak-Dzik, G.; Golab, G. *Polyhedron* **1994**, *13*, 1069−1075.
(3) Crawford, M. J.; Ellern, A.; Mayer, P. *Angew. Chem., Int. Ed.* **2005**, *44*, 7874−7878.
(4) Nocton, G.; Pecaut, J.; Mazzanti, M. *Angew. Chem., Int. Ed.* **2008**, *47*, 3040−3042.
(5) Turner, Z. R.; Bellabarba, R.; Tooze, R. P.; Arnold, P. L. *J. Am. Chem. Soc.* **2010**, *132*, 4050−4051.
(6) Arnold, P. L.; Liddle, S. T. *Chem. Commun.* **2005**, 5638−5640.
(7) Singh, U. P.; Tyagi, S.; Sharma, C. L.; Gomer, H.; Weyhermuller, T. *J. Chem. Soc., Dalton Trans.* **2002**, 4464−4470.
(8) Kumar, R.; Singh, U. P. *J. Mol. Struct.* **2008**, *875*, 427−434.

(9) Schumann, H.; Janiak, C.; Pickardt, J. *J. Organomet. Chem.* **1988**, *349*, 117−122.
(10) Evans, W. J.; Montalvo, E.; Champagne, T. M.; Ziller, J. W.; DiPasquale, A. G.; Rheingold, A. L. *J. Am. Chem. Soc.* **2008**, *130*, 16−17.
(11) Walter, M. D.; Weber, F.; Wolmershauser, G.; Sitzmann, H. *Angew. Chem., Int. Ed.* **2006**, *45*, 1903−1905.
(12) Evans, W. J.; Kozimor, S. A.; Ziller, J. W. *Science* **2005**, *309*, 1835−1838.
(13) King, D. M.; Tuna, F.; McInnes, E. J. L.; McMaster, J.; Lewis, W.; Blake, A. J.; Liddle, S. T. *Science* **2012**, *337*, 717−720.
(14) Melman, J.; Fitzgerald, M.; Freedman, D.; Emge, T.; Brennan, J. *J. Am. Chem. Soc.* **1999**, *121*, 10247−10248.
(15) Kornienko, A.; Emge, T.; Hall, G.; Brennan, J. *Inorg. Chem.* **2002**, *41*, 121−126.
(16) Kornienko, A. Y.; Emge, T. J.; Kumar, G. A.; Riman, R. E.; Brennan, J. G. *J. Am. Chem. Soc.* **2005**, *127*, 3501−3505.
(17) Banerjee, S.; Kumar, G. A.; Riman, R.; Emge, T. J.; Brennan, J. *J. Am. Chem. Soc.* **2007**, *129*, 5926−5931.
(18) Banerjee, S.; Huebner, L.; Romanelli, M. D.; Kumar, G. A.; Riman, R.; Emge, T. J.; Brennan, J. G. *J. Am. Chem. Soc.* **2005**, *127*, 15900−15906.
(19) Norton, K.; Banerjee, S.; Huebner, L.; Das, S.; Emge, T. J.; Brennan, J. G. *J. Chem. Soc., Dalton Trans.* **2010**, *39*, 6794−6800.
(20) Romanelli, M. D.; Kumar, G. A.; Riman, R. E.; Emge, T. J.; Brennan, J. G. *Angew. Chem.* **2008**, *47*, 6049−6051.
(21) Moore, B. F.; Kumar, G. A.; Tan, M. C.; Kohl, J.; Riman, R. E.; Brik, M.; Emge, T. J.; Brennan, J. G. *J. Am. Chem. Soc.* **2011**, *132*, 373−378.
(22) Kornienko, A.; Moore, B. F.; Kumar, G. A.; Tan, M. C.; Riman, R. E.; Brik, M. G.; Emge, T. J.; Brennan, J. G. *Inorg. Chem.* **2011**, *50*, 9184−9190.
(23) Kornienko, A.; Banerjee, S.; Kumar, G. A.; Riman, R. E.; Emge, T. J.; Brennan, J. G. *J. Am. Chem. Soc.* **2005**, *127*, 14008−14014.
(24) Melman, J.; Emge, T. J.; Brennan, J. G. *Inorg. Chem.* **1999**, *38*, 2117.
(25) Freedman, D.; Emge, T. J.; Brennan, J. G. *J. Am. Chem. Soc.* **1997**, *119*, 11112−11113.
(26) Melman, J.; Emge, T. J.; Brennan, J. G. *Chem. Commun.* **1997**, 2269−2270.
(27) Kornienko, A. Y.; Emge, T. J.; Brennan, J. G. *J. Am. Chem. Soc.* **2001**, *123*, 11933−11939.
(28) Fenske, D.; Anson, C. E.; Eichhoefer, A.; Fuhr, O.; Ingendoh, A.; Persau, C.; Richert, C. *Angew. Chem., Int. Ed.* **2005**, *44*, 5242−5246.
(29) Eichhoefer, A.; Olkowska-Oetzel, J.; Fenske, D.; Fink, K.; Mereacre, V.; Powell, A. K.; Buth, G. *Inorg. Chem.* **2009**, *48*, 8977−8984.
(30) Anson, C.; Eichhoefer, A.; Issac, I.; Fenske, D.; Fuhr, O.; Sevillano, P.; Persau, C.; Stalke, D.; Zhang, J. *Angew. Chem.* **2008**, *47*, 1326−1331.
(31) Fenske, D.; Langetepe, T. *Angew. Chem., Int. Ed* **2002**, *41*, 300−304.
(32) Ahlrichs, R.; Besinger, J.; Eichhofer, A.; Fenske, D.; Gbureck, A. *Angew. Chemie, Int. Ed* **2000**, *39*, 3929−3933.
(33) Fenske, D.; Bettenhausen, M. *Angew. Chemie, Int. Ed.* **1998**, *37*, 1291−1294.
(34) Behrens, S.; Bettenhausen, M.; Deveson, A. C.; Eichhoefer, A.; Fenske, D.; Lohde, A.; Woggon, W. *Angew. Chemie, Int. Ed.* **1996**, *35*, 2215−2218.
(35) Yang, L. X.; Xu, X.; Hao, L. Y.; Yang, X. F.; Tang, J. Y.; Xie, R. J. *Opt. Mater.* **2011**, *33*, 1695−1699.
(36) Mikami, M.; Kijima, N. *Opt. Mater.* **2010**, *33*, 145−148.
(37) Cho, I. H.; Anoop, G.; Suh, D. W.; Lee, S. J.; Yoo, J. S. *Opt. Mater. Express* **2012**, *2*, 1292−1305.
(38) Lu, F. C.; Guo, S. Q.; Yang, Z. P.; Yang, Y. M.; Li, P. L.; Li, X.; Liu, Q. L. *J. Alloys Compd.* **2012**, *521*, 77−82.
(39) Hirosaki, N.; Xie, R.; Takeda, T. *Mater. Integr.* **2010**, *23*, 5−7.
(40) Dierre, B.; Xie, R. J.; Hirosaki, N.; Sekiguchi, T. *J. Mater. Res.* **2007**, *22*, 1933−1941.
(41) Bruker-AXS. *SADABS, Bruker Nonius area detector scaling and absorption correction*; Bruker-AXS Inc.: Madison, WI, 2003.
(42) Sheldrick, G. M. *SHELXS86, Program for the Solution of Crystal Structures*; University of Göttingen: Germany, 1986.
(43) (a) Sheldrick, G. M. *Acta Crystallogr.* **2008**, *A64*, 112. (b) Sheldrick, G. M. *SHELXL97, Program for Crystal Structure Refinement*; University of Göttingen: Germany, 1997.
(44) Graphics programs: ORTEP-3 for Windows: Farrugia, L. J. *J. Appl. Crystallogr.* **1997**, *30*, 565. Burnett, M. N.; Johnson, C. K. *ORTEP-III: Oak Ridge Thermal Ellipsoid Plot Program for Crystal Structure Illustrations*, Oak Ridge National Laboratory Report ORNL-6895, 1996. Persistence of Vision Pty. Ltd., *Persistence of Vision Raytracer (Version 3.6)*; 2004.
(45) ICDD. *Powder Diffraction File*; Frank McClune, Ed.; International Centre for Diffraction Data, 12 Campus Boulevard, Newtown Square, Pennsylvania, U.S.A., 2003, pp 19073−3272.
(46) Ribas, J.; Escuer, A.; Monfort, M.; Vincente, R.; Cortes, R.; Lezama, L.; Rojo, T. *Coord. Chem. Rev.* **1999**, *193*−*5*, 1027−1068.
(47) Zi, G.; Yang, Q.; Mak, T. C. W.; Xie, Z. *Organometallics* **2001**, *21*, 2359−2361.
(48) Pi, C.; Wan, L.; Gu, Y.; Zheng, W.; Weng, L.; Chen, Z.; Wu, L. *Inorg. Chem.* **2008**, *47*, 9739−9741.
(49) Singh-Wilmot, M. A.; Kahhwa, I. A.; White, A. J. P.; Williams, D. J.; Lough, A. J. *Polyhedron* **2010**, *29*, 270−279.
(50) Berardini, M.; Emge, T. J.; Brennan, J. *J. Chem. Soc. Chem. Commun.* **1993**, 1537−1538.
(51) Freedman, D.; Melman, J.; Emge, T.; Brennan, J. *Inorg. Chem.* **1998**, *37*, 4162−4163.
(52) Zhou, X.; Ma, H.; Wu, Z.; You, X.; Xu, Z.; Huang, X. *J. Organomet. Chem.* **1995**, *503*, 11−13.
(53) Pernin, C. G.; Ibers, J. A. *Inorg. Chem.* **1997**, *36*, 3802−3803.
(54) Daniele, S.; Hubert-Pfalzgraf, L. G.; Hitchcock, P. B.; Lappert, M. F. *Inorg. Chem. Commun.* **2000**, *3*, 218−220.
(55) Sheng, J. Z.; Wen, G. J.; Cheng, W.; Yu, H. J.; Qi, S. *Jiegou Huaxue* **1990**, *9*, 140−144.
(56) Zhu, J. J.; Cheng, W. G.; Sheng, J. Z.; Qi, C. W. *Jiegou Huaxue* **1992**, *11*, 369−372.
(57) Boeyens, J. C. A.; de Villiers, J. P. R. *J. Cryst. Mol. Struct.* **1972**, *2*, 197−211.
(58) Zi, G.; Yang, Q.; Mak, T. C. W.; Xie, Z. *Organometallics* **2001**, *20*, 2359.
(59) Hubert-Pfalzgraf, L. G.; Daniele, S.; Bennaceur, A.; Daran, J. C.; Vaissermann, J. *Polyhedron* **1997**, *16*, 1223−1234.
(60) Wen, G. J.; Qi, S.; Yu, H. J.; Hua, L. Y. *Jiegou Huaxue* **1990**, *9*, 184−187.
(61) Gao, L. X.; Zhi, L. J.; Chen, J. S.; Hua, L. Y.; Zhi, L. G. *Jiegou Huaxue* **1991**, *10*, 60−66.
(62) Andrews, P. C.; Gee, W. J.; Junk, P. C.; Massi, M. *New J. Chem.* **2013**, *37*, 35−48.
(63) Romanelli, M.; Emge, T. J.; Brennan, J. G. *Acta Crystallogr. (E)* **2008**, *E64*, m987−m988.
(64) Norton, K.; Kumar, G. A.; Dilks, J. L.; Emge, T. J.; Riman, R. E.; Brik, M. G.; Brennan, J. G. *Inorg. Chem.* **2009**, *48*, 3573−3580.
(65) Freedman, D.; Emge, T.; Brennan, J. *Inorg. Chem.* **1999**, *38*, 4400−4404.
(66) Freedman, D.; Sayan, S.; Croft, M.; Emge, T.; Brennan, J. *J. Am. Chem. Soc.* **1999**, *121*, 11713−11719.
(67) Berardini, M.; Emge, T.; Brennan, J. G. *J. Am. Chem. Soc.* **1994**, *116*, 6941−6942.
(68) Banerjee, S.; Sheckelton, J.; Emge, T. J.; Brennan, J. G. *Inorg. Chem.* **2010**, *49*, 1728−1732.
(69) Banerjee, S.; Emge, T. J.; Brennan, J. G. *Inorg. Chem.* **2004**, *43*, 6307−6312.
(70) Kornienko, A.; Huebner, L.; Freedman, D.; Emge, T.; Brennan, J. *Inorg. Chem.* **2003**, *42*, 8476−8480.
(71) Lee, J. S.; Emge, T. J.; Brennan, J. G. *Inorg. Chem.* **1997**, *36*, 5064−5068.
(72) Berardini, M.; Emge, T.; Brennan, J. *Inorg. Chem.* **1995**, *34*, 5327−5334.

(73) Brewer, M.; Lee, J.; Brennan, J. G. *Inorg. Chem.* **1995**, *34*, 5919−5924.
(74) Huebner, L.; Kornienko, A.; Emge, T. J.; Brennan, J. G. *Inorg. Chem.* **2005**, *44*, 5118−5122.
(75) Thomson, R. K.; Cantat, T.; Scott, B. L.; Morris, D. E.; Batista, E. R.; Kiplinger, J. E. *Nat. Chem.* **2010**, *2*, 723−729.
(76) Muller, P.; Schroder, B.; Parkinson, J. A.; Kratochwil, N. A.; Coxall, R. A.; Parkin, A.; Parsons, S.; Sadler, P. J. *Angew. Chem., Int. Ed.* **2003**, *42* (3), 335−339.
(77) Klapotke, T. M.; Krumm, B.; Mayer, P.; Schwab, I. *Angew. Chem., Int. Ed.* **2003**, *42*, 5843−5846.

dx.doi.org/10.1021/ic400359x | *Inorg. Chem.* 2013, 52, 6021−6027